

FULL WAVE BIE ANALYSIS OF TRAVELLING WAVES IN UNBIASED / VELOCITY SATURATED FET STRUCTURES WITH LINEARLY CONTROLLED CURRENT DENSITY

Werner Schroeder*, Werner Prost†, and Ingo Wolff*

*Dept. of Electromagnetic Theory and Engineering, † Solid State Electronics Department
Duisburg University, D-47048 Duisburg, Germany

ABSTRACT

The Hybrid Wave Boundary Integral Equation method is applied to analyze wave propagation along the width of a linearized InGaAs/InAlAs HFET model with accurate description of all geometrical details. Special consideration is given to the influence of operating conditions on propagation characteristics by introducing separate linear models for unbiased operation, channel depletion and velocity saturated operation. Results are given for the gate and drain mode in the passive device and for the mixed mode in presence of a linearly controlled channel current density.

INTRODUCTION

Accurate prediction of the millimeter wave performance of HFETs and MESFETs is a topic of growing interest. One aspect of the “dilemma of models” for this purpose is the gap between physics based device simulation and circuit level device characterization. The former is involved with a basically 2-dimensional, quasi-static device model. Voltages and currents are assumed to be in-phase and position independent along the device width. Circuit level device models, on the other hand, are in terms of scattering parameters at external ports, relative to the connecting transmission line system.

The models required to fill this gap are (a) a full-wave model of the extrinsic device which yields the scattering matrix between the external ports and reference planes on the internal gate-source-drain electrode system, (b) full wave analysis of wave propagation along the latter and (c) an adequate concept to connect a physics based transport simulation to the EM field solution. The present paper is concerned with (b). Analysis of the device internal EM field has long been recognized as a transmission line problem (e.g. [1, 2]). Early full-wave investigations of canonical FET structures (rectangular electrodes on layered conducting/isolating media) have shown that slow wave propagation may result in a non-negligible phase shift along the device (e.g. [3, 4]). Beyond passive device models, a landmark in full-wave 3-d de-

vice simulation has recently been set by [5] where a FDTD scheme is coupled with a hydrodynamic transport model. Results presented in [5] confirm that despite of nonlinearity the transmission line picture is consistent with the main features of wave propagation along the device.

Most previously studied geometries, however, bear little resemblance with the cross-section of a state of the art HFET (Fig. 1a). Since slow wave propagation is too a high degree governed by the distribution of the current density within the field penetrated, non-ideal conductors, full-wave analysis must accurately account for finite conductivity and shape details of the conductors (Fig. 1c) in order to be more meaningful than a quasi-static analysis. In the framework of a linearized device description we further have to distinguish between models appropriate for (i) the unbiased device with

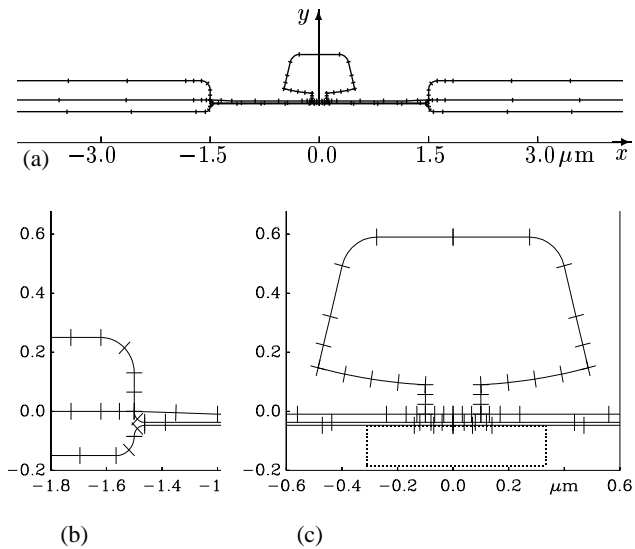


Fig. 1: (a) Cross-section of the symmetric InGaAs/InAlAs HFET structure with indication of discretization intervals on subregion boundaries; (b) detail of the model for the transition from the contact region to the 10 nm channel; (c) detail of the 0.2 μ m gate. Dotted region delineates *intrinsic device*. See also Table 1.

low field channel mobility, (ii) channel depletion and (iii) velocity saturated operation with zero AC mobility but field controlled channel current density. For all three cases we address the analysis of EM wave propagation along the device width as an eigenvalue problem for the fundamental modes supported by the respective model structure. The eigenvalue problems are solved by means of the Hybrid Wave Boundary Integral Equation Method (BIEM) [6] which has been extended for the present study to allow for subregions with a non-locally field controlled current density.

DEVICE MODEL

Fig. 1 shows the cross-section of the symmetric InGaAs / InAlAs HFET structure whose parasitics are subject of the present investigation. In reality its extension along the x -axis is more than $5 \cdot 10^3$ times the smallest dimension which is to be represented in the model (10 nm channel thickness). To keep the dimensional ratio within reasonable limits source and drain electrodes have been cut off at $|x| = 5 \mu\text{m}$ in the model structure. The actual contour of the T-shaped gate (Fig. 1c) is modeled after an electron micrography. The whole cross-section is described as an arrangement of linear, isotropic and piecewise homogeneous media as detailed in Table 1. The region within the dotted box in Fig. 1c will be referred to as the *intrinsic device* below. Three different simple linear models are considered for the intrinsic device:

For the *cold FET model* we assume a constant conductivity throughout the channel according to the measured low field sheet resistance. In the *depleted FET model* the channel conductivity is set to zero for $|x| \leq 0.3 \mu\text{m}$. In the *active FET model* it is assumed that velocity saturation occurs in a hot field region, $|x| \leq 50 \text{ nm}$, symmetrically about the origin of the x -axis. This simplification allows to maintain the symmetry of the structure. The hot field region is assigned zero AC conductivity but it supports a controlled current den-

Table 1: Geometrical and material parameters of the model structures. See Fig. 1 for remaining dimensions.

subregion	thickness	dielectric constant	conductivity
“air”	∞	1.0	–
“source”	250 nm	1.0	$\sigma_s = 31.25 \frac{\text{S}}{\mu\text{m}}$
“gate”	(see Fig. 1c)	1.0	$\sigma_g = 31.25 \frac{\text{S}}{\mu\text{m}}$
“drain”	250 nm	1.0	$\sigma_d = 31.25 \frac{\text{S}}{\mu\text{m}}$
“barrier” ^a	27.5(+10) nm	12.33	–
“channel”	10 nm	13.7	$\sigma_c = 0.6 \frac{\text{S}}{\mu\text{m}}$
“contact”	150 nm	13.7	$\sigma_c = 0.6 \frac{\text{S}}{\mu\text{m}}$
“substrate”	30 μm	12.33	–

^aThe region between gate and channel; 10 nm gate recess.

sity $\mathbf{J}_c = \frac{1}{t} \rho_c v_{\text{sat}} \mathbf{e}_x$, where t denotes channel thickness and ρ_c the average sheet channel charge density under the gate. The latter is approximated by the average $\langle D_y \rangle$ of the electrical flux density on the bottom face of the gate electrode, $|x| \leq 100 \text{ nm}$. Within the BIE formulation (see below) the flux density is obtained as $D_y = \frac{j}{\omega} \left(\frac{\partial}{\partial x} H_z + \gamma H_x \right)$. The “impressed” channel current density is thus described as a non-local, linear functional of the even part of the field only, a simplification which again aims at maintaining symmetry.

The model of the remaining passive structure is, however, rigorous with the exception of some not easily accessible physical details, e.g. the contact resistance between the source (drain) metalization and the alloyed region. The conductivity of this region has been set equal to the channel conductivity of $6 \cdot 10^5 \text{ S/m}$ in the present model.

FIELD THEORETICAL APPROACH

The EM field problem is posed as an eigenvalue problem for the complex effective permittivity $\epsilon_{r,\text{eff}} := -\gamma^2/k_0^2$ of the fundamental modes supported by the respective model structure. The solution is obtained with the Hybrid Wave Boundary Integral Equation Method [6]. For treatment of the *active FET model* the method has been extended to allow for inclusion of a controlled current density \mathbf{J}_c in addition to the conduction current density $\sigma \mathbf{E}$. With reference to the local system of normal, tangential and axial unit vectors ($\mathbf{n}, \mathbf{t}, \mathbf{a}$) on each subregion boundary, the BIE systems for a single, homogeneously filled subregion of the device cross-section is

$$\mathbf{K}[\mathbf{aH}] - \frac{h^2}{j\omega\mu} \mathbf{G}[t\mathbf{E}] - \frac{\gamma}{j\omega\mu} \mathbf{G}\left[\frac{\partial}{\partial s} \mathbf{aE}\right] = -\mathbf{Q}[\text{div } \mathbf{a} \times \mathbf{J}_c] - \mathbf{G}[t\mathbf{J}_c], \quad (1)$$

$$\mathbf{K}[\mathbf{aE}] + \frac{h^2}{(\sigma + j\omega\epsilon)} \mathbf{G}[t\mathbf{H}] + \frac{\gamma}{(\sigma + j\omega\epsilon)} \mathbf{G}\left[\frac{\partial}{\partial s} \mathbf{aH}\right] = -j\omega\mu\mathbf{Q}[\mathbf{aJ}_c] + \frac{\gamma}{(\sigma + j\omega\epsilon)} \mathbf{G}[\mathbf{nJ}_c]. \quad (2)$$

\mathbf{K} and \mathbf{G} denote boundary integral operators acting on the tangential ($t\mathbf{E}, t\mathbf{H}, t\mathbf{J}_c$), normal (\mathbf{nJ}_c) or axial (\mathbf{aH}, \mathbf{aE}) field components and \mathbf{Q} is a domain integral operator. Their kernels are given by the free space Green’s function and its normal derivative. $h^2 := \gamma^2 - j\omega\mu(\sigma + j\omega\epsilon)$ denotes the transverse wavenumber. The simultaneous system of BIEs for all subregions, mutually coupled by the common tangential field components along their interfaces, describes the allowed fields within the structure. Unless $h^2 = 0$ for some subregion, it is equivalent to Maxwell’s equations for linear, isotropic and piecewise homogeneous media. In our present model, where the “impressed” channel current density \mathbf{J}_c is divergence free and purely transverse, both domain integral

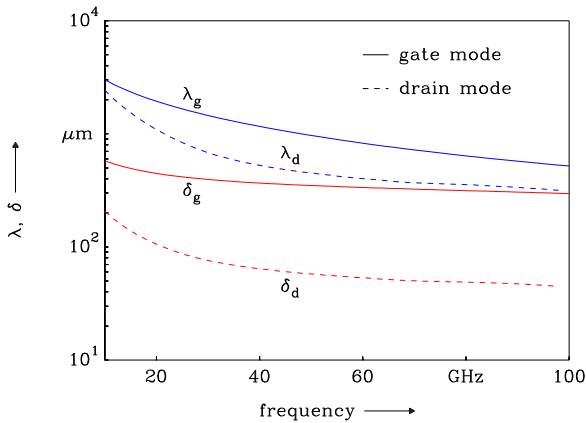


Fig. 2: Gate and drain mode wavelength and decay length for the cold FET model.

operators vanish. Furthermore, since \mathbf{J}_c is defined as a linear functional of the remaining unknowns the global system of BIEs is homogeneous and has nontrivial solutions only for the eigenvalues of the propagation constant or, equivalently, $\epsilon_{r,\text{eff}}$. To solve the problem numerically, the BI operators are discretized by expanding the unknown axial and transverse tangential field components on each subregion boundary into 2nd order B-splines. These expansion functions extend over 3 elements of the boundary partitions shown in Fig. 1. Exploiting symmetry approx. 300 expansion functions are required for each model. The residual of the global operator equation is tested using the Method of Least Squares with Intermediate Projection [7]. The resultant matrix operator is subject to singular value decomposition to locate the eigenvalues of $\epsilon_{r,\text{eff}}$ as minima of the residual of the global system. The search strategy was to obtain first the (real) eigenvalues for the case $\sigma_s = \sigma_c = \sigma_d = \infty$ and $\sigma_c = 0$ at a fixed frequency, then trace $\epsilon_{r,\text{eff}}$ through parameter space up to the final values and then follow its evolution over frequency. It must be noted that the numerical effort for the second step is considerable since $|\epsilon_{r,\text{eff}}|$ changes over two orders magnitude as a function of σ_c .

RESULTS

Cold FET model. Fig. 2 shows the wavelength and the decay length $\delta := 1/\alpha$ for the gate and drain mode between 10 GHz and 100 GHz. The electrical length of a 100 μm device at 100 GHz amounts to more than 60° for the gate mode and almost 120° for the drain mode which also shows very strong attenuation. Boundary values of selected field components are shown in Fig. 3 for the gate mode and in Fig. 4 for the drain mode, both at 50 GHz. Figs. 3a and b illustrate that the reversal of the axial current density is not in phase over the cross-section, an observation which underlines the importance of a rigorous treatment of the electrodes. The relevant wave propagation effects are in fact observed within the electrodes due to their large complex permittivity $\epsilon - j \frac{\sigma}{\omega}$. The transverse electric field in the barrier and channel region, on the other hand, is essentially a gradient field. From the magnitude of the axial magnetic field component we conclude that the voltage measured around an arbitrary loop in the region $|x| \leq 1.5 \mu\text{m}$, $-3 \mu\text{m} \leq y \leq 0 \mu\text{m}$ is less than 5×10^{-4} times the gate-source or drain-source voltage up to 100 GHz. The maximum of the magnitude ratio between the axial and transverse electric field components in the channel region is approx. 5% at 100 GHz. These figures are of interest when evaluating the potential merits of full-wave solvers over the traditional Possion solvers in a physics based simulation of the intrinsic device.

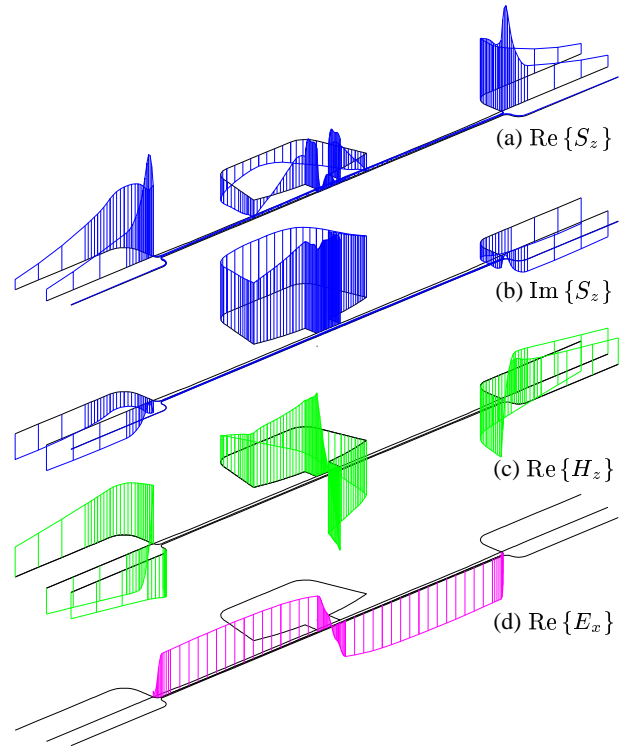


Fig. 3: Boundary values of selected field components for the cold FET gate mode at 50 GHz; (a,b) real and imaginary part of axial current density, (c) real part of axial magnetic field on electrode boundaries, (d) tangential electric field on the upper face of the channel. Subfigures are scaled separately.

As expected both modes propagate much faster if the channel is depleted. The drain mode attenuation constant is about one order of magnitude less then for the cold FET model. Wavelengths and decay lengths are given in Fig. 5.

Depleted Channel model. As expected both modes propagate much faster if the channel is depleted. The drain mode attenuation constant is about one order of magnitude less then for the cold FET model. Wavelengths and decay lengths are given in Fig. 5.

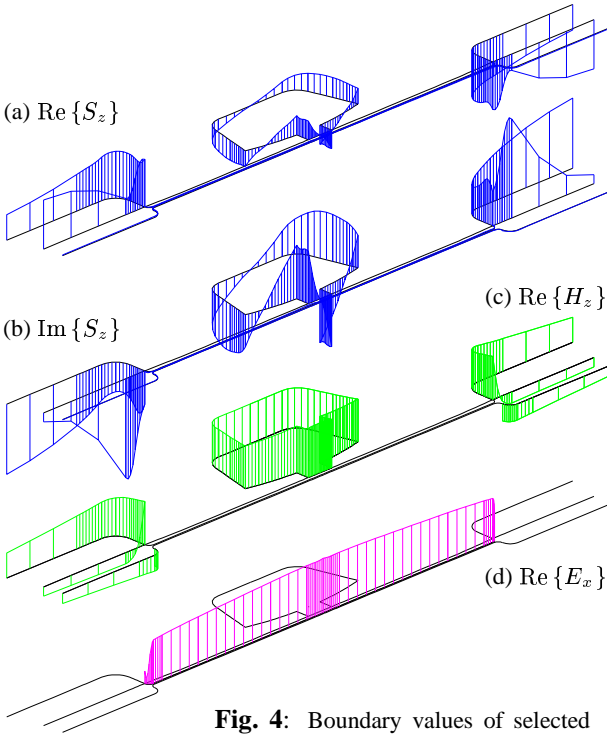


Fig. 4: Boundary values of selected field components for the cold FET drain mode at 50 GHz; See caption of Fig. 3.

Active FET model. As a consequence of symmetry and the above mentioned simplifications which neglect any influence of the odd mode fields on the controlled channel current density, the drain mode is not affected by the “active” coupling. The even mode is replaced by a mixed mode whose propagation constant is (within numerical accuracy) that of the gate mode in absence of coupling. For space limitations we restrict to the most interesting piece of information which

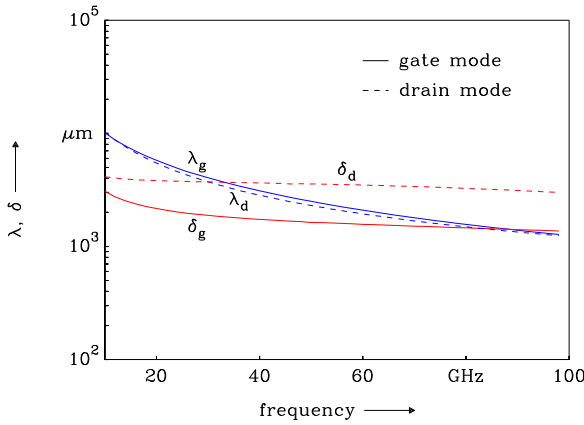


Fig. 5: Gate and drain mode wavelength and decay length for the depleted channel model.

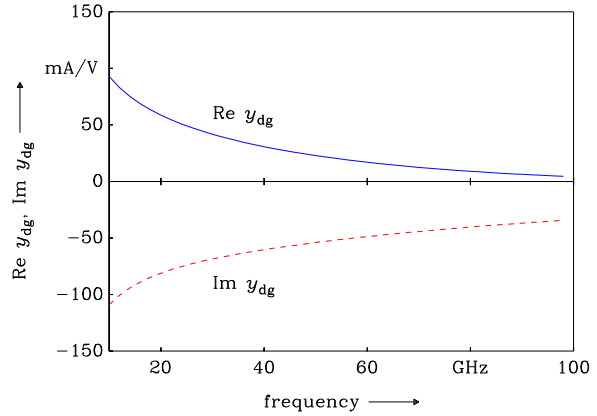


Fig. 6: Excitation of the drain mode current wave by the gate mode voltage for $v_{\text{sat}} = 10^5$ m / s.

can be drawn from our simple model, i.e. the ratio $y_{\text{dg}} = i_{\text{d}}/v_{\text{g}}$ of the odd field current $i_{\text{d}} = \frac{1}{2}(\oint_{\text{d}} \mathbf{t} \mathbf{H} \, ds - \oint_{\text{s}} \mathbf{t} \mathbf{H} \, ds)$ to the even field voltage $v_{\text{g}} = \frac{1}{2}(\oint_{\text{g} \rightarrow \text{s}} \mathbf{t} \mathbf{E} \, ds + \oint_{\text{g} \rightarrow \text{d}} \mathbf{t} \mathbf{E} \, ds)$, with the latter integrals taken along the substrate/air interface. The frequency dependence of y_{dg} is shown in Fig. 6 scaled to a saturation velocity of $v_{\text{sat}} = 10^5$ m / s.

REFERENCES

- [1] R. L. Kuvas, “Equivalent circuit model of FET including distributed gate effects,” *IEEE Trans. Electron Devices*, vol. 27, no. 6, pp. 1193–1195, 1980.
- [2] W. Heinrich, “Distributed equivalent-circuit model for traveling-wave fet design,” *IEEE Trans. Microwave Theory Tech.*, vol. 35, pp. 487–491, May 1987.
- [3] Y. Fukuoka and T. Itoh, “Analysis of slow-wave phenomena in coplanar waveguide on a semiconductor substrate,” *Electronics Letters*, vol. 18, pp. 589–590, 1982.
- [4] W. Heinrich and M. Hartnagel, “Field-theoretic analysis of wave propagation on FET electrodes including losses and small-signal amplification,” *Int. J. Electronics*, vol. 58, no. 4, pp. 613–627, 1985.
- [5] M. A. Alsunaidi, S. M. S. Imtiaz, and S. M. El-Ghazaly, “Electromagnetic wave effects on microwave transistors using a full-wave time domain model,” *IEEE Trans. Microwave Theory Tech.*, vol. 44, pp. 799–808, June 1996.
- [6] W. Schroeder and I. Wolff, “A hybrid-mode boundary integral equation method for normal- and superconducting transmission lines of arbitrary cross-section,” *Int. J. Microwave and Millimeter-Wave CAE*, vol. 2, pp. 314–330, Oct. 1992.
- [7] W. Schroeder and I. Wolff, “The origin of spurious modes in numerical solutions of electromagnetic field eigenvalue problems,” *IEEE Trans. Microwave Theory Tech.*, vol. 42, pp. 644–653, Apr. 1994.